Aspirin promotes RSL3-induced ferroptosis by suppressing mTOR/SREBP-1/SCD1-mediated lipogenesis in *PIK3CA*-mutatnt colorectal cancer

Hao Chen [a,1], Qinqin Qi [b,1], Nan Wu [a], Ying Wang [a], Qian Feng [a], Rong Jin [a,**], Lei Jiang [b,*]

[a] *Department of Gastroenterology, The First Affiliated Hospital of Wenzhou Medical University, Wenzhou, 325000, China*
[b] *Central Laboratory, The First Affiliated Hospital of Wenzhou Medical University, Wenzhou, 325000, China*

ARTICLE INFO

ABSTRACT

Ferroptosis, a new form of regulated cell death triggered by the iron-dependent peroxidation of phospholipids, is associated with cellular metabolism, redox homeostasis, and various signaling pathways related to cancer. Aspirin is a widely used non-steroidal anti-inflammatory drug (NSAID) and has been reported to show therapeutic benefit in cancers harboring oncogenic *PIK3CA*, which encodes the catalytic p110α subunit of phosphoinositide 3-kinase (PI3K). In this study, we found that aspirin sensitized cancer cells harboring oncogenic activation of *PIK3CA* to ferroptosis induction. Mechanistically, aspirin inhibited protein kinase B (AKT)/mammalian target of rapamycin (mTOR) signaling, suppressed downstream sterol regulatory element-binding protein 1 (SREBP-1) expression, and attenuated stearoyl-CoA desaturase-1 (SCD1)-mediated lipogenesis of monounsaturated fatty acids, thus promoting RSL3-induced ferroptosis in colorectal cancer (CRC) cells. Moreover, genetic ablation of SREBP-1 or SCD1 conferred cancer cells greater sensitivity to ferroptosis induction. Conversely, ectopic expression of SREBP-1 or SCD1 restored ferroptosis resistance in CRC cells and abolished the effect of aspirin on RSL3-induced cytotoxicity. Additionally, the synergistic effects of aspirin and RSL3 were confirmed in a xenograft mouse model. The combined use of aspirin and RSL3 resulted in significant tumor suppression. Our work demonstrated that aspirin enhanced the cytotoxic effect of RSL3 in *PIK3CA*-mutant cancers, and the combination of aspirin and ferroptosis inducer displayed promising therapeutic effects in cancer treatment.

1. Introduction

CRC is a serious health burden worldwide, ranking third in incidence and second in mortality among all cancers [1]. As the dreadful disease becomes symptomatic at an advanced stage, primary prevention and organized screening programs are of great importance [2–4]. However, once the early critical stage is missed, CRC is difficult to control and caused approximately 935,000 deaths last year [5]. Despite great progress, such as the development of new targeted drugs [6] or immune checkpoint inhibitors [7,8] since the 2000s, the overall prognosis of patients with advanced or recurrent CRC is relatively unsatisfactory [9].

Aspirin (acetylsalicylic acid) is the cornerstone of modern therapies because of its important role in analgesia and cardiovascular prophylaxis [10,11]. In addition, epidemiological studies indicate that daily use of low-dose aspirin is associated with a reduced risk of cancer development [12,13], suggesting that it can be used as part of adjuvant therapy. Inhibition of cyclooxygenase (COX) enzymes, particularly COX-2, and reduced production of inflammatory mediators are thought to be the main mechanisms of tumor control [14]. In addition, other COX-independent mechanisms, such as inhibition of NF-kappaB [15], Wnt/beta-catenin [16,17], and the mTOR signaling pathway [18,19] are involved. A recent study showed that aspirin use is associated with a significant improvement in survival in patients with mutant *PIK3CA* CRC but not in their wild-type counterparts [20], suggesting that the benefits of aspirin treatment vary in patients with different *PIK3CA* statuses.

Ferroptosis is a newly discovered form of regulated cell death characterized mainly by iron accumulation, redox system imbalance and lipid peroxidation [21]. In mammalian cells, the system xc/glutathione peroxidase 4 (GPX4) axis plays a crucial role in limiting lipid

---

peroxidation [22]. Pharmacological blockade of key enzymes such as GPX4 (e.g. RSL3) or deprivation of substrates such as cysteine can effectively trigger ferroptosis [23,24]. In addition to GPX4, recent studies have shown that ferroptosis suppressor protein 1 (FSP1) suppresses ferroptosis by producing reductive coenzyme Q (CoQ) to limit the accumulation of phospholipid peroxides [25]. In contrast, lipid peroxidation is positively regulated by other enzymes such as acyl-CoA synthetase long-chain family member 4 (ACSL4) or cytochrome P450 oxidoreductase (POR) [26,27]. Unlike other programmed cell deaths such as autophagy and apoptosis, ferroptosis is morphologically and biochemically unique [28]. Because it has far-reaching effects on various pathophysiological conditions, such as tumor suppression [29], neurodegenerative diseases [30], and ischemia-reperfusion injury [31,32], ferroptosis has received considerable attention in recent years. Cancers with mesenchymal characteristics have been found to be much more susceptible to ferroptosis [33–35]. In addition, many small-molecule drugs, such as sulfasalazine or sorafenib, that target ferroptosis are used as a strategy to treat a variety of cancers [36]. Recent evidence suggests that ferroptosis may offer a new therapeutic strategy for CRC [37–39]. Our previous study showed that cetuximab, which is approved for the treatment of metastatic CRC with wild-type Kirsten rat sarcoma (KRAS), promoted RSL3-induced ferroptosis by suppressing the NRF2/HO-1 pathway in KRAS-mutant CRC [37]. The natural product β-elemene has been described as a novel ferroptosis inducer, and combined treatment with β-elemene and cetuximab inhibits KRAS-mutant CRC cell growth by inducing ferroptosis [38]. Xia et al. reported that talaroconvolutin A (TalaA) suppresses CRC cells via ferroptosis, and may be a new and potentially effective drug candidate for CRC therapy [39]. Recently, oncogenic activation of PI3K/AKT/mTOR signaling was reported to render cancer cells resistant to ferroptosis [40], suggesting that drugs targeting PI3K in combination with ferroptosis inducers may achieve better therapeutic outcomes in the treatment of *PIK3CA*-mutant CRC.

Here, we found that CRC harboring the oncogenic *PIK3CA* mutation might benefit from aspirin therapy in combination with the ferroptosis inducer RSL3. Mechanistically, aspirin suppressed the PI3K/AKT/mTOR pathway, thereby promoting the sensitivity of CRC cells to ferroptosis by inhibiting downstream SREBP-1/SCD1-mediated lipogenesis. Our study provides an experimental basis for the combined use of aspirin and ferroptosis inducers for the treatment of *PIK3CA*-mutant CRC.

2. Materials and methods

2.1. Cell lines

Human cancer cell lines, including DLD-1, HCT 116, HepG2, PANC-1, and AGS, were obtained from the Shanghai Institute of Cell Biology, Chinese Academy of Sciences (CAS; Shanghai, China). All cells were cultured in RPMI-1640 or DMEM media supplemented with 10% fetal bovine serum (FBS; Thermo Fisher Scientific, MA, USA), 100 μg/mL streptomycin and 100 units/mL penicillin in a humidified atmosphere with 5% CO_2 at 37 °C according to the recommendations of the American Tissue Culture Collection (ATCC).

2.2. Reagents and antibodies

RSL3 (#SML2234), aspirin (#A2093), OA (#O1383), POA (#P9417), PA (#P0500) and SA (#S4751) were purchased from Sigma-Aldrich (Darmstadt, Germany). Ferrostatin-1 (Fer-1, #HY100579), Z-VAD-FMK (#HY16658B), 3-Methyladenine (3-MA, #HY19312), MHY1485 (#HY-B0795) and Rapamycin (#HY10219) were obtained from MedChemExpress (NJ, USA). Primary antibodies against AKT (#4691), phosphorylated AKT (p-Akt; #4060), mTOR (#2983), phosphorylated mTOR (p-mTOR; #5536), p70S6K (#2708), phosphorylated p70S6K (p-p70S6K; #9204), 4E-BP1 (#9644), phosphorylated 4E-BP1 (p-4E-BP1; #2855) and SCD1 (#2794) were purchased from Cell

Signaling Technology (MA, USA). SREBF1 antibody (#14088-1-AP) was obtained from Proteintech (IL, USA). The antibodies against Ki67 (#ab16667) and 4-HNE (#ab46545) were purchased from Abcam (MA, USA).

2.3. Cell viability assay

Cells were seeded in 96-well plates at optimal cell density (3000–5000 per well) and incubated overnight at 37 °C. After cells were subjected to various treatments as indicated, 10 μL of Cell Counting Kit-8 (CCK-8; #CK04, Dojindo Laboratories, Japan) solution was added to medium. Following 3 h incubation, absorbance was determined at 450 nm using a microplate reader (Bio-Tek, USA).

2.4. Lipid reactive oxygen species (ROS) assay

The level of Lipid ROS was detected by C11-BODIPY 581/591 (#D3861, Thermo Fisher Scientific). After cells were exposed to the indicated treatments, 5 μM of C11-BODIPY 581/591 dye was added and incubated at 37 °C for 30 min. All results were analyzed using FlowJo V10 software.

2.5. Crystal violet staining

For crystal violet staining, cells (20,000 per well) were seeded in 24-well plates and treated with aspirin or RSL3 at the indicated concentration. After 2 days of incubation, cells were stained with crystal violet staining solution (0.05%, w/v) for 30 min before washing and air-drying.

2.6. Malondialdehyde (MDA) assay

The levels of intracellular MDA were measured using a Lipid Peroxidation MDA Assay Kit (#A003-4-1, Nanjing Jiancheng, China) according to the manufacturer's instructions.

2.7. Intracellular iron assay

The level of intracellular Ferrous ion was determined using FerroOrange dye (#F374, Dojindo Laboratories). Cells were seeded and exposed to the indicated treatments. After treatment, FerroOrange (1:2000, v/v) was added to the cells and the cells were incubated at 37 °C for 30 min. Fluorescence images were acquired using a confocal microscope.

2.8. Western blot analysis

Cells with different treatments as described in each experiment were lysed in RIPA buffer (#89901, Thermo Fisher Scientific) supplemented with protease inhibitor. A total of 20–30 μg of cell lysates were subjected to SDS-polyacrylamide gel electrophoresis (PAGE) gels and then electrophoretically transferred to polyvinylidene difluoride membranes (Millipore, MA, USA). After incubation in 5% skim milk for 2 h at room temperature, the membranes were incubated with the indicated primary antibodies at 4 °C overnight. After washing three times with Tris-buffered saline and Tween-20 (TBST) buffer, the blots were then reprobed with the HRP-conjugated secondary antibodies for 1 h at room temperature. The membranes were subjected to enhanced chemiluminescence and visualized using a Gel Doc 2000 (CA, USA).

2.9. Small interfering RNA (siRNA) and plasmid transfection

The siRNAs targeting the *SREBF1* or *SCD1* gene were purchased from GenePharma (Shanghai, China). The sequences of the siRNAs are as follows: si*SREBF1* #1 (sense: 5′- CGGAGAAGCUGCCUAUCAA -3′); si*S-REBF1* #2 (sense: 5′- CCACAACGCCATCGAG AAA -3′); si*SCD1* #1

(sense: 5′- GCACAUCAACUUCACCACA -3′); si*SCD1* #2 (sense: 5′-GGAGAAACAUCAUCCUUAUUU -3′). The plasmids containing the insert SREBP-1a (pcDNA3.1-2×FLAG-SREBP-1a, #26801) or SREBP-1c (pcDNA3.1-2×FLAG-SREBP-1c, #26802) were obtained from Addgene. The plasmid containing the SCD1 insert and the control vector were purchased from GenePharma. Transfection of cells was performed using Lipofectamine 3000 reagent (Thermo Fisher Scientific) according to the instructions.

2.10. Immunohistochemistry (IHC)

Xenograft tumor tissue was fixed, dehydrated, embedded, and sectioned (3.5 μm). The slides were stained with Ki67 (1:200), 4-HNE (1:50), SREBP-1 (1:200) and SCD1 (1:200) antibodies. The staining index was calculated by multiplying the intensity value (negative = 0, weak = 1, moderate = 2, or strong = 3) by the percentage value of positively stained cells (< 5% = 0, >5 to ≤ 25% = 1, >25 to ≤ 50% = 2, >50 to ≤ 75% = 3, >75% = 4) independently by two pathologists.
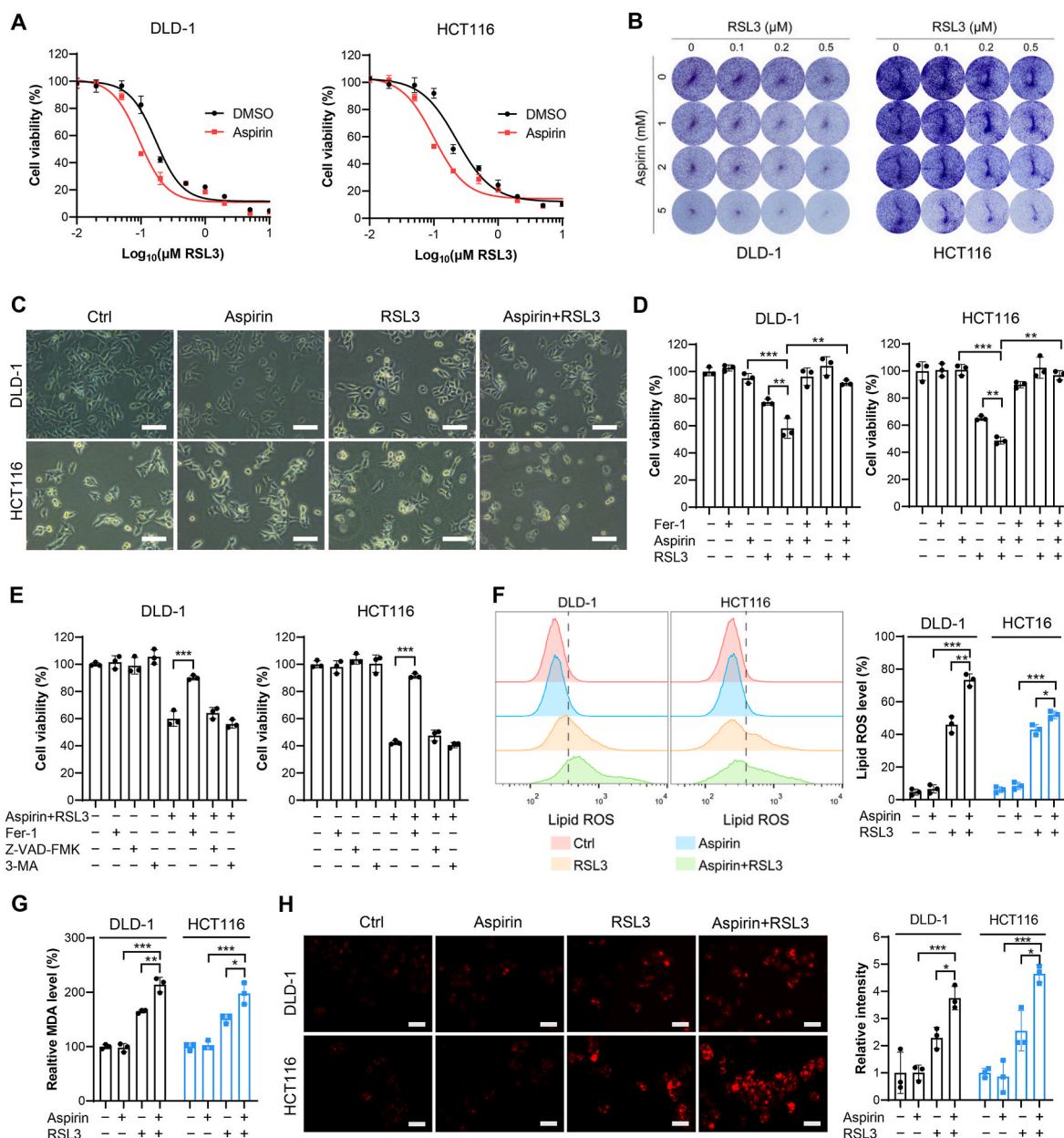

Fig. 1. Aspirin promotes RSL3-induced ferroptosis in *PIK3CA*-mutant CRC cells. (A) DLD-1 and HCT116 cells were treated with different concentration of RSL3 (0, 0.01, 0.02, 0.05, 0.1, 0.2, 0.5, 1, 2, 10 μM) combined with DMSO or aspirin (2 mM) for 24 h, and cell viability was measured by CCK-8 assays. (B) Violet staining was performed with the indicated concentration of aspirin and RSL3 combination treatment. (C) The changes in cell morphology were observed after treatment with aspirin (2 mM), RSL3 (0.1 μM) or their combination in DLD-1 and HCT116 cells. Scale bar, 100 μm. (D) Cell viability was measured in DLD-1 and HCT116 cells treated with aspirin (2 mM), RSL3 (0.1 μM),or the combination in the presence or absence of Fer-1 for 24 h. (E) Cell viability was measured in DLD-1 and HCT116 cells treated with aspirin (2 mM) and RSL3 (0.1 μM) combination in the presence of with Fer-1 (1 μM), Z-VAD-FMK (10 μM), or 3-MA (1 mM) for 24 h. (F–H) The levels of lipid ROS detected with C11-BODIPY 581/591 (F), MDA detected with the MDA assay kit (G), and ferrous ion detected with FerroOrange dye (H), in DLD-1 and HCT116 cells treated with aspirin (2 mM), RSL3 (0.1 μM) or the combination for 24 h. Scale bar, 50 μm *, $P < 0.05$; **, $P < 0.001$; ***, $P < 0.001$. (For interpretation of the references to color in this figure legend, the reader is referred to the Web version of this article.)

2.11. In vivo tumor xenograft study

Male BALB/c nude mice (5–6 weeks old) were purchased from Shanghai SLAC Laboratory Animal Co., Ltd. (Shanghai, China). All animal experiments were approved by the Laboratory Animal Ethics Committee of the First Affiliated Hospital of Wenzhou Medical University. An equal number (5×10^6) of DLD-1 cells suspended in 200 μL phosphate-buffered saline (PBS) were injected subcutaneously into the right flank of each mouse. Six days after inoculation, the mice were randomly divided into four groups (6 mice/group): 1) the control group, 2) the RSL3 group, 3) the aspirin group, and 4) the RSL3 + aspirin group. Both RSL3 (5 mg/kg) and aspirin (100 mg/kg) were administered by intraperitoneal injection in a volume of 100 μL once per day. The mice weight and tumor volume were measured every other day. Tumor volume was calculated as $0.5 \times \text{length} \times \text{width}^2$. On day 22 after treatment, all mice were sacrificed and tumors were removed and weighed.

2.12. Statistical analysis

All analyses were performed using GraphPad Prism 8.0 software (CA, USA). Data were expressed as means ± SD. Student's *t*-test analysis was used to determine differences between the means of two groups, whereas one-way ANOVA analysis for multiple groups. $P < 0.05$ was considered statistically significant.

3. Results

3.1. Aspirin promotes RSL3-induced ferroptosis in PIK3CA-mutant CRC cells

To validate the effect of aspirin on *PIK3CA*-mutant CRC cells, DLD-1 and HCT116 cells were exposed to different concentrations of aspirin. We found that aspirin inhibited cell growth in dose- and time-dependent manners (Fig. S1A). To determine the combined effect of aspirin and RSL3, a Bliss independence model was established to calculate the synergistic effect (Fig. S1B). Surprisingly, the combined administration of aspirin and RSL3 showed strong synergism in terms of anti-proliferative effects (Figs. S1B and 1A). This synergistic phenomenon was verified using crystal violet staining (Fig. 1B). Combined administration of aspirin and RSL3 also resulted in low cell viability when observed under a light microscope (Fig. 1C).

As RSL3 is a potent inducer of ferroptotic cell death, we hypothesized that the effects of ferroptosis were enhanced by the addition of aspirin. Consistent with our expectation, the inhibition of cell growth by the combination treatment was reversed by the application of the ferroptosis inhibitor Fer-1, but not by the autophagy inhibitor 3-MA or the apoptosis inhibitor Z-VAD-FMK (Fig. 1D and E). In addition, the levels of lipid ROS, intracellular ferrous ion and MDA, three widely used ferroptosis indicators, were measured in the DLD-1 and HCT116 cells. The levels of lipid ROS and MDA increased significantly after the combination treatment with aspirin and RSL3 (Fig. 1F and G). Moreover, DLD-1 and HCT116 cells showed higher fluorescence in the combination group than in the RSL3 group (Fig. 1H). Interestingly, aspirin itself did not affect the levels of lipid ROS, MDA, or iron fluorescence intensity in either DLD-1 or HCT116 cells, suggesting that aspirin may enhance RSL3-induced cell death in *PIK3CA*-mutant CRC cells. We also validated the combined effect of aspirin and RSL3 in *PIK3CA* wild type CRC cells (SW480, SW620, and Lovo). The addition of aspirin did not significantly enhance ferroptosis induced by RSL3 (Fig. S1C). Taken together, these results suggest that aspirin administration promotes RSL3-induced ferroptosis in *PIK3CA*-mutant CRC cells.

3.2. Combination treatment with aspirin and RSL3 suppresses the AKT/mTORC1 signaling axis in PIK3CA-mutant CRC cells

To determine whether the increased sensitivity of ferroptosis to aspirin treatment was due to the suppression of the PI3K/AKT/mTOR pathway in *PIK3CA*-mutant CRC cells, we analyzed the associated protein levels. Indeed, we found that the protein levels of AKT, p-AKT, p-mTOR and mTOR decreased sharply in the combination treatment group (Fig. 2A and S2A). In addition, the phosphorylation of mTORC1 substrate 4E-binding protein 1 (4E-BP1) reduced by aspirin and RSL3 (Fig. 2B and S2B). Next, the mTORC1 activator MHY1485 and inhibitor rapamycin were used to further investigate the effects of mTORC1 on the regulation of ferroptosis. The results showed that pretreatment with MHY1485 conferred DLD-1 and HCT116 cells resistance to the ferroptosis inducer even in the presence of aspirin (Fig. 2C), whereas rapamycin sensitized cancer cells to ferroptosis (Fig. 2D). Furthermore, MHY1485 significantly decreased RSL3-induced lipid ROS, MDA and Fe^{2+} levels, whereas rapamycin increased RSL3-induced lipid ROS, MDA and Fe^{2+} levels in LDD-1 and HCT116 cells (Fig. 2E–G). The above results suggest that the activity of mTORC1 is responsible for the sensitivity of ferroptosis in *PIK3CA*-mutant CRC cells.

3.3. Aspirin sensitizes PIK3CA-mutant CRC cells to RSL3-induced ferroptosis by inhibiting SREBP-1 activity

SREBP-1 has recently been identified as a downstream target of mTORC1 [41]. Therefore, we investigated whether SPEBP-1 played a key role in modulating ferroptosis sensitivity. Consistent with our expectations, the levels of both total SREBP-1 and its mature form (mSREBP-1) decreased to a high extent by the combination treatment than by RSL3 only (Fig. 3A). Small interfering RNAs (si*SREBF1* #1 and si*SREBF1* #2) were used to knock down the expression of SREBP-1, and the knockdown effects were verified by western blotting (Fig. 3B). We found that inhibition of SREBP-1 expression sensitized DLD-1 and HCT116 cells to ferroptosis induction, and cell death was reversed by the ferroptosis inhibitor Fer-1 (Fig. 3C). In contrast, ectopic expression of the mature form of SREBP-1 (SREBP-1a or SREBP-1c) resulted in resistance to ferroptosis (Fig. 3D and E). The above evidence suggests that aspirin promotes ferroptosis by suppressing SREBP-1 expression.

3.4. Aspirin sensitizes PIK3CA-mutant CRC cells to ferroptosis by suppressing SCD1 expression

As SREBP-1 regulates transcription of several genes related to lipid synthesis, RT-PCR was performed to assess the mRNA expression of downstream target genes, including *ACC*, *ACLY*, *SCD1* and *FASN*. We found that the mRNA expression of SCD1 decreased more markedly than other genes (Fig. 4A). Combination treatment with aspirin and RSL3 also significantly decreased SCD1 protein expression (Fig. 4B and S3). To investigate whether inhibition of SCD1 triggers activation of ferroptosis, siRNAs targeting *SCD1* were transfected into DLD-1 and HCT116 cells and the efficacy of knockdown was verified by western blotting (Fig. 4C). Knockdown of SCD1 sensitized DLD-1 and HCT116 cells to ferroptosis induction, and the effects were abolished by the ferroptosis inhibitor Fer-1 (Fig. 4D). The pro-ferroptotic effects were confirmed by the accumulation of lipid ROS, intracellular iron, and lipid peroxides (Fig. 4E–G).

3.5. Ectopic expression of SCD1 renders PIK3CA-mutant CRC cells resistant to ferroptosis induction

To further confirm the role of SCD1 in ferroptosis process, SCD1 was overexpressed in *PIK3CA*-mutant CRC cells (Fig. 5A). Overexpression of SCD1 in DLD-1 and HCT116 cells reversed the inhibition of cell growth induced by the combination treatment with RSL3 and aspirin or knocking down *SREBF1* (Fig. 5B). At the same time, the levels of lipid ROS, MDA, and Fe^{2+} decreased dramatically upon overexpression of SCD1 (Fig. 5C–E). Similar to Fer-1 treatment, overexpression of SCD1 restored cell viability inhibited by the combination treatment with RSL3 and aspirin and knockdown of SREBP-1 (Fig. 5F).
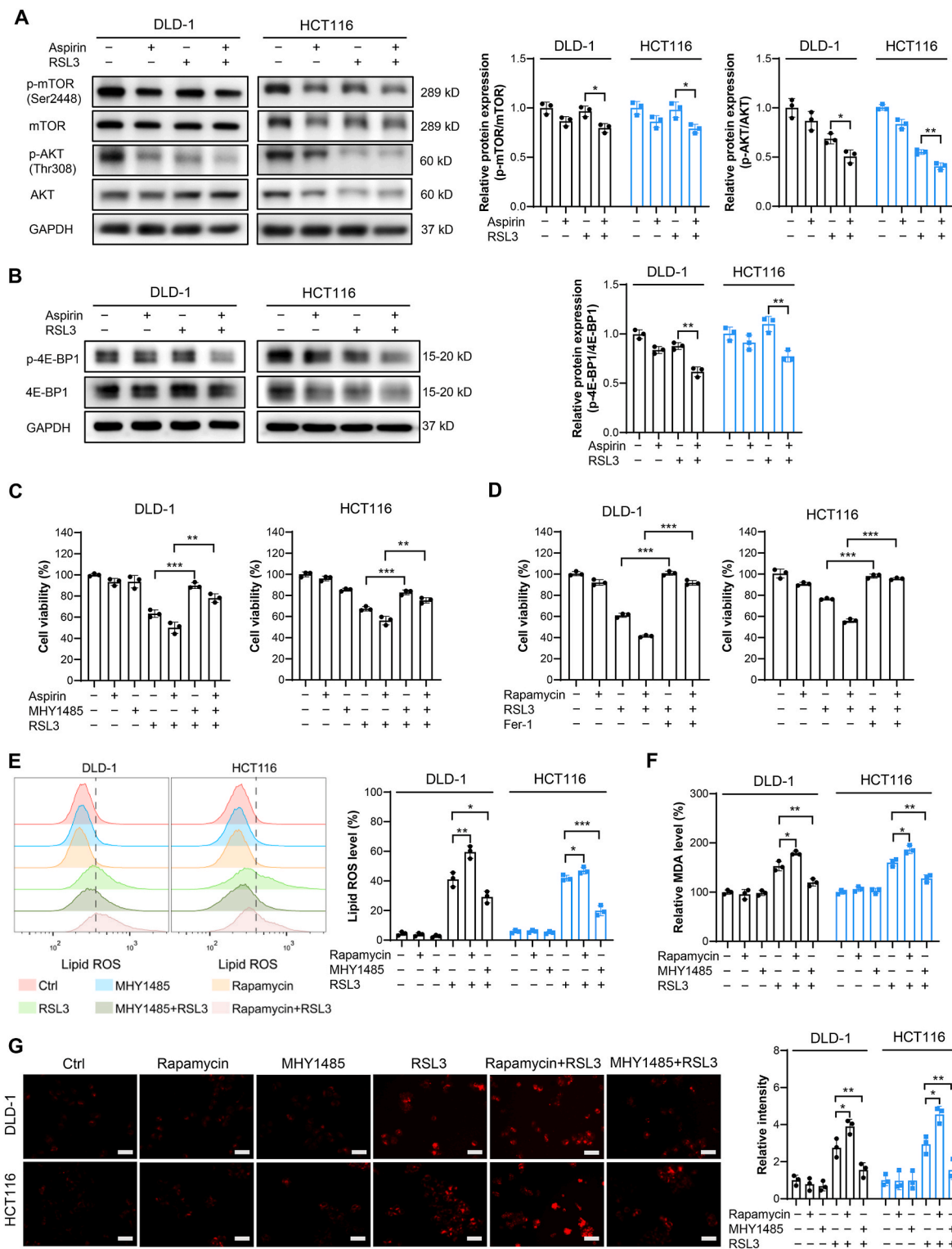
Fig. 2. Combination treatment with aspirin and RSL3 suppresses the AKT/mTORC1 signaling axis in *PIK3CA*-mutatnt CRC cells. (A–B) The protein levels of AKT, p-AKT, mTOR, 4E-BP1, p-4E-BP1 were detected in DLD-1 and HCT116 cells treated with aspirin (2 mM), RSL3 (0.1 μM), or their combination for 24 h. **(C)** DLD-1 and HCT116 cells were pretreated with MHY1485 (2 μM) for 6 h and then exposed to aspirin (2 mM), RSL3 (0.1 μM) or the combination for 24 h. Cell viability was determined by CCK-8 assays. **(D)** DLD-1 and HCT116 cells were pretreated with rapamycin (50 nM) for 6 h and then exposed to RSL3 (0.1 μM) or Fer-1 (1 μM) for 24 h. Cell viability was determined by CCK-8 assays. **(E–G)** DLD-1 and HCT116 cells were pretreated with rapamycin (50 nM) or MHY1485 (2 μM) for 6 h and then treated with RSL3 (0.1 μM) for 24h. The levels of lipid ROS detected with C11-BODIPY 581/591**(E)**, MDA detected with the MDA assay kit **(F)**, and ferrous ion detected with FerroOrange dye **(G)**. Scale bar, 50 μm *, $P < 0.05$; **, $P < 0.001$; ***, $P < 0.001$.
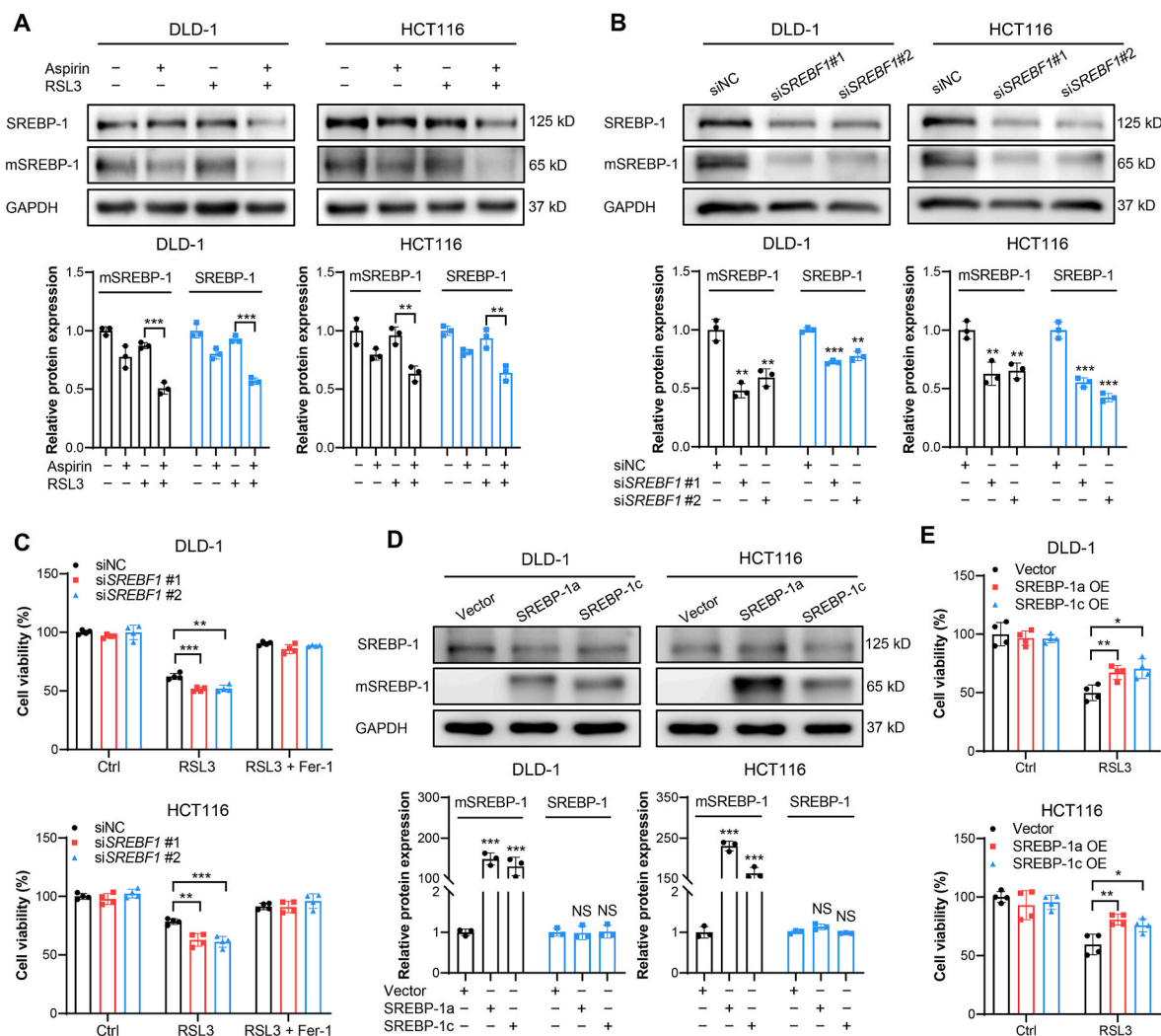
Fig. 3. Aspirin sensitizes *PIK3CA*-mutant CRC cells to RSL3-induced ferroptosis through inhibiting SREBP-1 activity. (A) The protein levels of SREBP-1 and mSREBP-1 were detected by Western blotting in DLD-1 and HCT116 cells treated with aspirin (2 mM), RSL3 (0.1 μM), or the combination for 24 h. **(B)** The protein levels of SREBP-1 and mSREBP-1 were detected in DLD-1 and HCT116 cells transfected with siNC or si*SREBF1*. (C) DLD-1 and HCT116 cells transfected with si*SREBF1* were treated with RSL3 (0.1 μM) for 24 h and the cell viability was measured by CCK-8 assays. (D) The protein levels of SREBP-1 and mSREBP-1 were detected in DLD-1 and HCT116 cells transfected with vectors expressing SREBP-1a or SREBP-1c. (E) DLD-1 and HCT116 cells overexpressing SREBP-1a or SREBP-1c were treated with RSL3 (0.1 μM) for 24 h and the cell viability was measured. *, $P < 0.05$; **, $P < 0.001$; ***, $P < 0.001$.

SCD1 is an important lipid desaturase that converts saturated fatty acids (SFAs) to monounsaturated fatty acids (MUFAs) [42]. Therefore, MUFA oleic acid (18:1, OA) and palmitoleic acid (16:1, POA) as well as SFA stearic acid (18:0, SA) and palmitic acid (16:0, PA) were supplemented in the experiment. We found that the addition of OA or POA rather than SA or PA protected DLD-1 and HCT116 cells from RSL3-induced ferroptosis, independent of addition of aspirin (Fig. 5G). Taken together, these results suggest that aspirin enhances RSL3-induced ferroptosis in *PIK3CA*-mutant CRC cells by inhibiting SCD1-mediated MUFA production.

3.6. The antitumor efficacy of combined aspirin and RSL3 therapy in a human CRC xenograft model

To further investigate the anticancer therapeutic potential of simultaneous treatment with aspirin and RSL3 *in vivo*, a DLD-1 xenograft model was established in nude mice. Six days after tumor inoculation, the mice were treated with vehicle, aspirin (100 mg/kg), RSL3 (5 mg/kg), or a combination of both. As shown in Fig. 6A and B, tumor growth was significantly slower in the combination groups than in the groups treated with aspirin or RSL3 alone. The tumor weight was also

significantly lower in the combination group than in the other groups (Fig. 6C). Meanwhile, MDA levels significantly increased in the tumor of the combination group (Fig. 6D). Fig. 6E shows that body weight remained stable during the treatments, indicating that the treatments were well tolerated. In addition, after simultaneous treatment with aspirin and RSL3, the Ki67 proliferation index significantly decreased compared to that in the groups treated with aspirin or RSL3 alone (Fig. 6F). The accumulation of lipid peroxides was also confirmed by IHC analysis of 4-HNE, another indicator of oxidative stress (Fig. 6F). Moreover, the levels of SREBP-1 and SCD1 decreased significantly in the combination treatment group compared with the RSL3 group, indicating that the synergistic effects promoted the induction of tumor ferroptosis (Fig. 6F). Overall, these *in vivo* results showed that aspirin enhanced RSL3-induced ferroptosis via tumor suppression by inhibiting the SREBP-1/SCD1 pathway. Taken together, these results show that the combined use of aspirin and ferroptosis induction shows therapeutic potential for the treatment of *PIK3CA*-mutant CRC.

4. Discussion

In the current study, we found that aspirin promoted the sensitivity
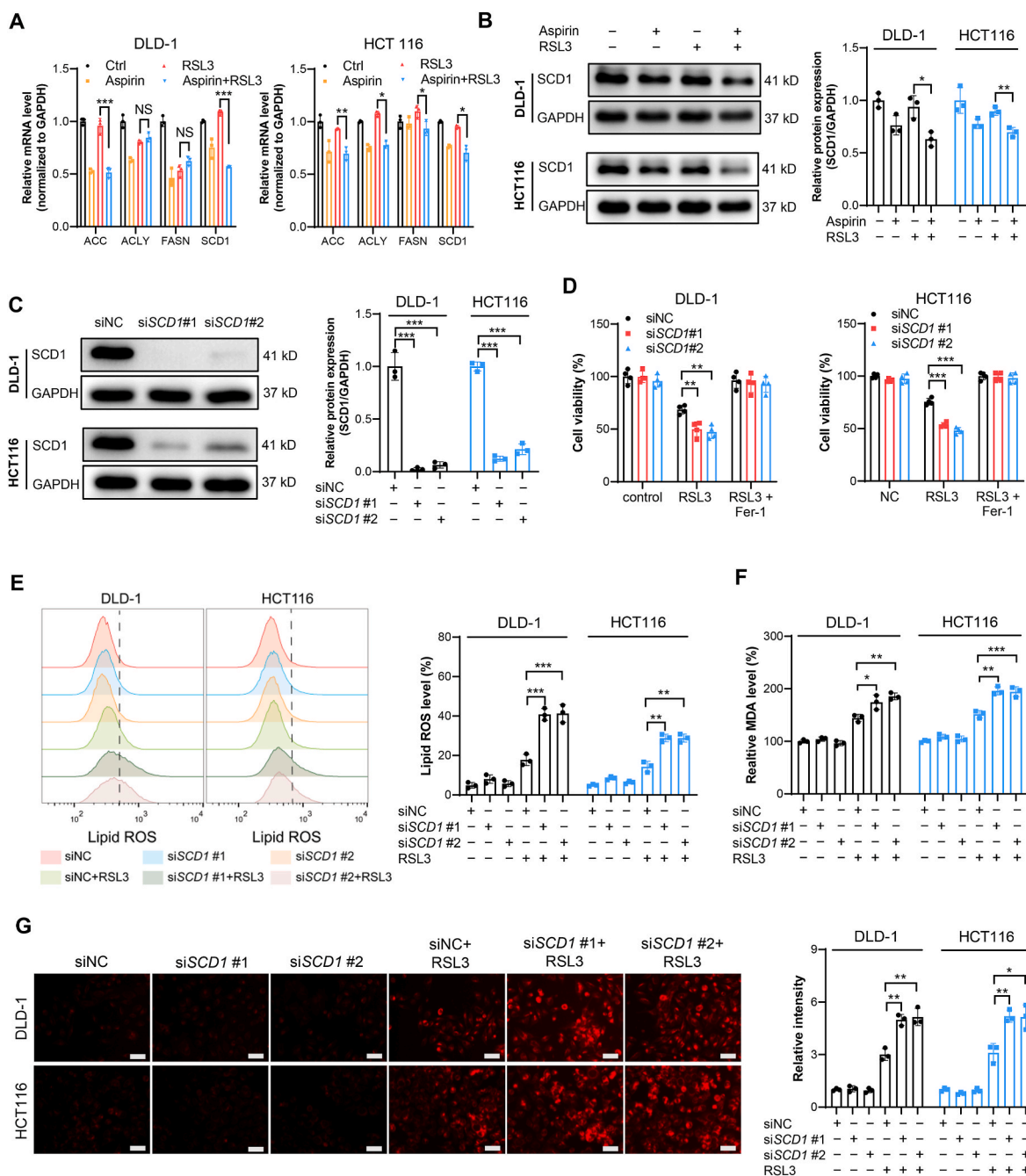
Fig. 4. Aspirin sensitizes *PIK3CA*-mutant CRC cells to ferroptosis by suppressing SCD1 expression. (A) The mRNA levels of ACC, ACLY, FASN, and SCD1 were detected by real time PCR in DLD-1 and HCT116 cells treated with aspirin (2 mM) and RSL3 (0.1 μM) for 24 h. **(B)** The protein levels of SCD1 were detected in DLD-1 and HCT116 cells treated with aspirin (2 mM), RSL3 (0.1 μM), or the combination for 24 h. **(C)** The protein levels of SCD1 were detected in DLD-1 and HCT116 cells transfected with si*SCD1*. **(D)** DLD-1 and HCT116 cells were transfected with si*SCD1* and then treated with RSL3 (0.1 μM) for 24 h. Cell viability was measured by CCK-8 assays. **(E–G)** DLD-1 and HCT116 cells were transfected with si*SCD1* and then treated with RSL3 (0.1 μM) for 24 h. The levels of lipid ROS detected with C11-BODIPY 581/591**(E)**, MDA detected with the MDA assay kit **(F)**, and ferrous ion detected by FerroOrange dye **(G)**. Scale bar, 50 μm *, $P < 0.05$; **, $P < 0.001$; ***, $P < 0.001$.

of *PIK3CA*-mutant CRC cells to RSL3-induced ferroptosis by inhibiting the AKT/mTORC1 axis and SREBP-1/SCD1-mediated lipogenesis of MUFA (Fig. 7). Although it is used clinically as an antipyretic analgesic, aspirin has shown therapeutic effects on primary tumors and metastatic neoplasms [43,44]. Aspirin has been reported to directly disrupt the mTOR-Raptor interaction and enhance the anticancer effects of sorafenib [19]. Moreover, aspirin has shown stronger suppression of *PIK3CA*-mutant breast cancers than their wild-type counterparts by activating AMPK signaling, suppressing mTOR activity, and inducing

autophagy [45].

The PI3K/AKT/mTOR pathway plays a critical role in regulating cell proliferation, survival and metabolism [46]. Somatic mutations in *PIK3CA* have been detected in approximately 20% of all CRC cases [47], leading to increased PI3K and downstream AKT activity and promotion of tumor progression. Although oncogenic mutations in *PIK3CA* or its hyperactivation are common in CRC, small molecules targeting the PI3K/AKT/mTOR pathway have yielded little benefits in clinical trials owing to the emergence of acquired resistance and dose-dependent
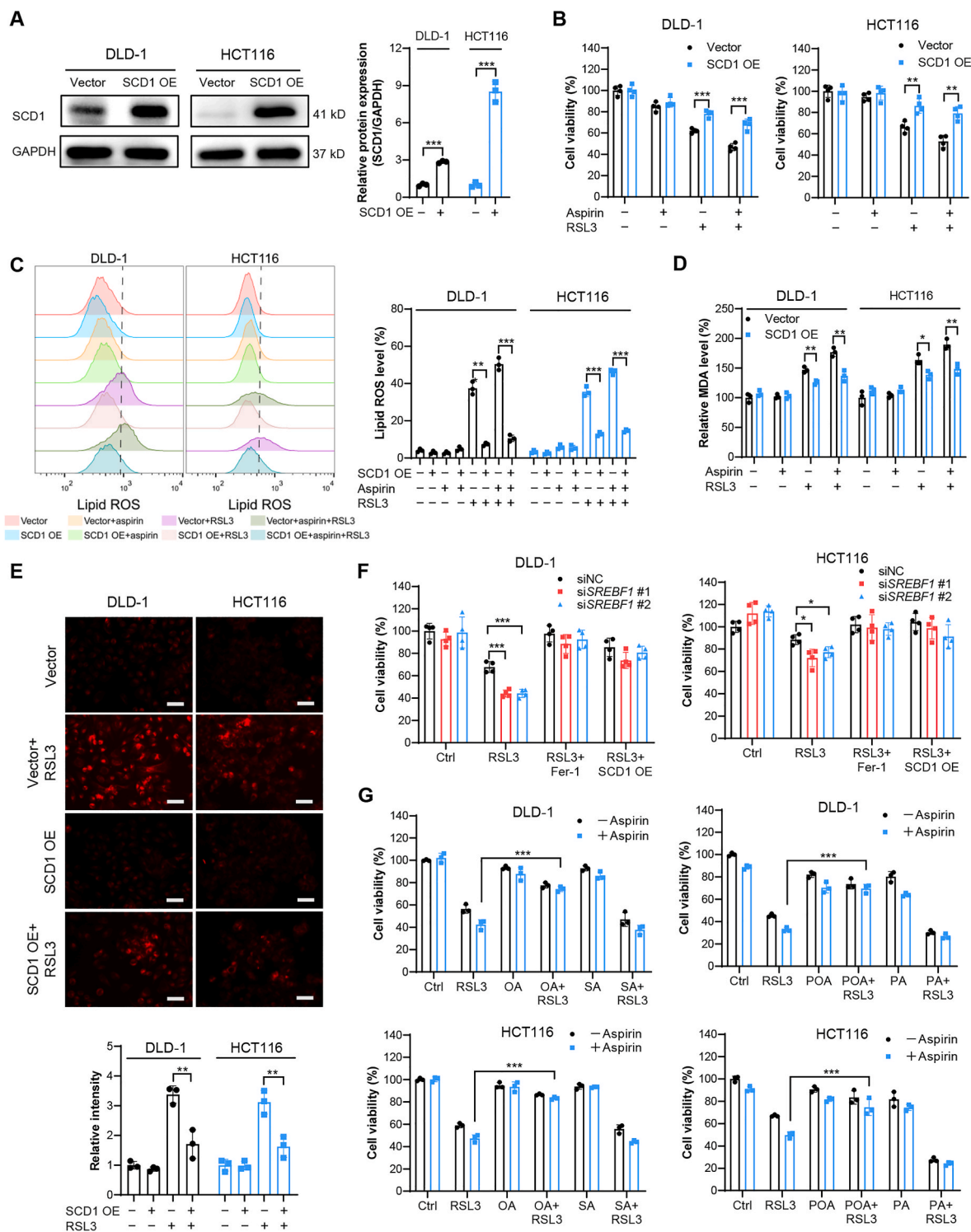
Fig. 5. Ectopic expression of SCD1 renders *PIK3CA*-mutant CRC cells resistant to ferroptosis induction. (A) The protein levels of SCD1 were detected in DLD-1 and HCT116 cells transfected with SCD1 overexpression plasmids. **(B)** DLD-1 and HCT116 cells with SCD1 overexpression were treated with RSL3 (0.1 μM) for 24 h. Cell viability was measured by CCK-8 assays. **(C–E)** The levels of lipid ROS detected by C11-BODIPY 581/591 **(C)**, MDA detected by the MDA assay kit **(D)**, and ferrous ion detected by FerroOrange dye **(E)**, in RSL3 (0.1 μM)-treated DLD-1 and HCT116 cells with SCD1 overexpression. Scale bar, 50 μm. **(F)** DLD-1 and HCT116 cells transfected with si*SREBF1* were treated with RSL3 (0.1 μM) and SCD1 overexpression plasmid. Cell viability was measured by CCK-8 assays. **(G)** DLD-1 and HCT116 cells were treated with RSL3 (0.1 μM), OA (100 μM), SA (100 μM), POA (100 μM) or PA (100 μM), with simultaneous treatments of Aspirin (2 mM) for 24 h. The cell viability was measured by CCK-8 assays. *, $P < 0.05$; **, $P < 0.001$; ***, $P < 0.001$.

toxicities [48]. The goal of finding new therapeutic strategies has taken on greater significance. Our results showed that the combination treatment with aspirin and RSL3 suppressed the AKT/mTORC1 signaling axis in *PIK3CA*-mutant CRC cells. COX-2 expression is significantly associated with Akt phosphorylation in epithelial ovarian cancer [49] and breast cancer [50]. Uddin S et al. showed that inhibition of COX-2 impairs the phosphorylation of AKT, leading to inhibition of cell growth and induction of apoptosis, and aspirin treatment inhibits the
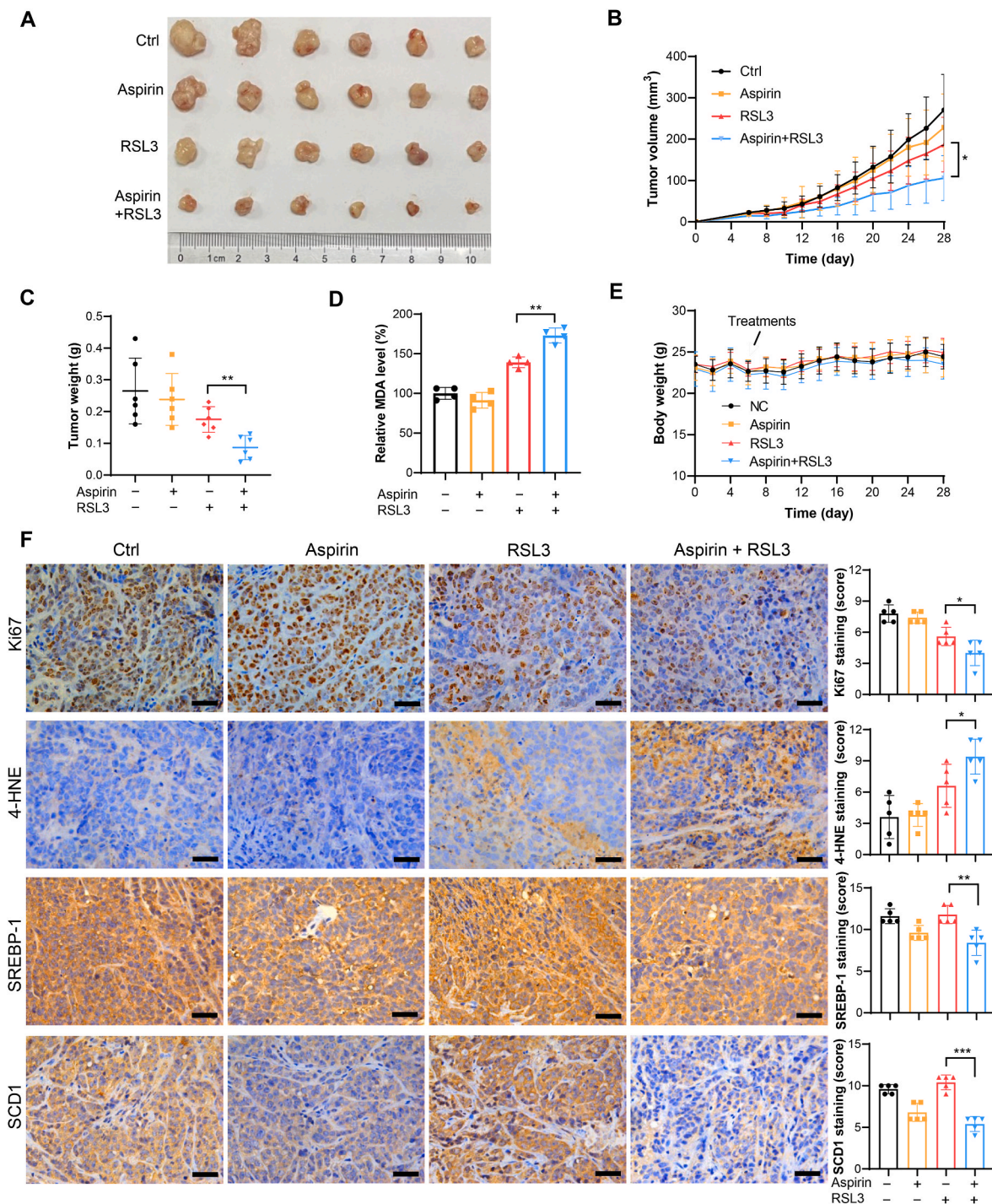
Fig. 6. The antitumor efficacy of combined aspirin and RSL3 therapy in a human CRC xenograft model. DLD-1 cells were injected subcutaneously into the right flank of nude mice. Six days after inoculation, mice received daily intraperitoneal RSL3 (5 mg/kg), aspirin (100 mg/kg), or the combination of the two drugs (n = 6). **(A)** Tumor images in different groups. **(B)** Tumor volume was measured every 2 days. **(C)** Tumor weight in four groups. **(D)** The levels of intracellular MDA were measured in different treatment groups. **(E)** The body weight of mice was measured every 2 days after the xenograft mouse model was established. **(F)** The expressions of Ki67, 4-HNE, SREBP-1, and SCD1 were determined by immunohistochemical staining, and the staining score was calculated. Scale bar, 40 μm *, $P < 0.05$; **, $P < 0.001$; ***, $P < 0.001$.

growth of MDAH2774 tumor cells in nude mice via down-regulation of COX-2 and AKT activity [49].

mTORC1 is a downstream molecule of PI3K-AKT signaling and is frequently deregulated in cancer [51]. Recent studies have shown that mTORC1 acts as a negative regulator of ferroptosis [52]. It has been reported that mTORC1 protects cardiomyocytes from excessive iron accumulation and therefore inhibits ferroptosis [53]. In addition,

mTORC1 mediates cystine-induced GPX4 synthesis [54]. Our work here showed that aspirin-induced suppression of mTORC1 further inhibits SREBP-1/SCD1-mediated MUFA production. Aljohani et al. demonstrated that SCD1 deficiency mediates activation of mTORC1, and therefore causes endoplasmic reticulum stress [55], showing that SCD1 may in turn regulate cellular metabolism by modulating mTORC1 activity.
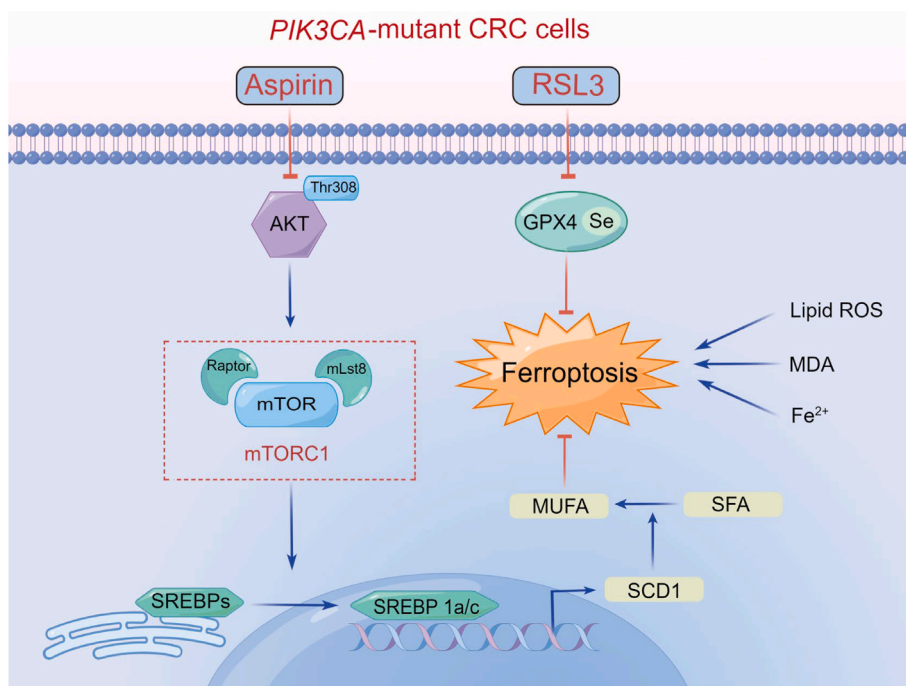
Fig. 7. Graphical summary of the mechanism by which aspirin promotes RSL3-induced ferroptosis by inhibiting the mTOR/SREBP-1/SCD1 axis.

SREBPs are a family of transcription factors that regulate the promoter of genes involved in lipid homeostasis and glucose metabolism in response to various metabolic stress [41,56]. The three SREBP isoforms, SREBP-1a and SREBP-1c, both encoded by *SREBF1*, and SREBP-2, encoded by *SREBF2*, have different roles in lipid synthesis [57–60]. Emerging evidence suggests that SREBP-1, including SREBP-1a and SREBP-1c, is an important link between tumor metabolism and oncogenic signaling. Critical genes in the lipogenesis pathway, such as acetyl-CoA carboxylase (*ACC*), ATP citrate lyase (*ACLY*), fatty acid synthase (*FASN*), and stearoyl-CoA desaturase (*SCD1*) are the main targets of SREBP-1 [61]. Moreover, SREBP-1 has been confirmed to be a downstream protein of the PI3K/AKT/mTOR signaling pathway. In this study, we found that aspirin inhibited the activity of mSREBP-1 and SCD1 and suppressed the synthesis of MUFA, thereby curbing the occurrence of ferroptosis [62]. SCD1 has been reported to protect lung and gastric cancers from ferroptosis [63,64]. Knockdown of SCD1 sensitized CRC cells to ferroptosis induction, whereas overexpression of SCD1 rendered CRC cells resistant to ferroptosis induction and restored cell viability inhibited by the combination treatment with RSL3 and knockdown of SREBP-1. Magtanong et al. reported that exogenous MUFA inhibits ferroptosis in an ACSL3-dependent manner [65]. These results demonstrate not only the role of unsaturated fatty acids in the regulation of ferroptosis, but also the relationship between SREBP-1 and SCD1 in the development of ferroptosis.

Here, we demonstrated that aspirin promoted ferroptosis in cancer cells harboring malignant mutation of PI3K, providing valuable insights into future ferroptosis-inducing cancer therapies. Our findings provide a theoretical basis for combining aspirin with ferroptosis inducers in the treatment of CRC and highlight the need for clinical trials to evaluate their potential chemotherapeutic effects.

Declaration of competing interest

The authors have no conflicts of interest to disclose. Fig. 7 is created using Figdraw (www.figdraw.com).

Data availability

Data will be made available on request.

Appendix A. Supplementary data

Supplementary data to this article can be found online at https://doi.org/10.1016/j.redox.2022.102426.

References

[1] H. Sung, J. Ferlay, R.L. Siegel, M. Laversanne, I. Soerjomataram, A. Jemal, et al., Global cancer statistics 2020: GLOBOCAN estimates of incidence and mortality worldwide for 36 cancers in 185 countries, Ca - Cancer J. Clin. 71 (3) (2021) 209–249.
[2] E. Dekker, P.J. Tanis, J.L.A. Vleugels, P.M. Kasi, M.B. Wallace, Colorectal cancer, Lancet 394 (10207) (2019) 1467–1480.
[3] E.H. Schreuders, A. Ruco, L. Rabeneck, R.E. Schoen, J.J. Sung, G.P. Young, et al., Colorectal cancer screening: a global overview of existing programmes, Gut 64 (10) (2015) 1637–1649.
[4] U. Ladabaum, J.A. Dominitz, C. Kahi, R.E. Schoen, Strategies for colorectal cancer screening, Gastroenterology 158 (2) (2020) 418–432.
[5] N. Keum, E. Giovannucci, Global burden of colorectal cancer: emerging trends, risk factors and prevention strategies, Nat. Rev. Gastroenterol. Hepatol. 16 (12) (2019) 713–732.
[6] B.V. Jensen, J.V. Schou, M. Yilmaz, H.H. Johannesen, K. Skougaard, D. Linnemann, et al., Cetuximab plus irinotecan administered biweekly with reduced infusion time to heavily pretreated patients with metastatic colorectal cancer and related RAS and BRAF mutation status, Int. J. Cancer 148 (10) (2020) 2542–2556, https://doi.org/10.1002/ijc.33448.
[7] M.J. Overman, R. McDermott, J.L. Leach, S. Lonardi, H.J. Lenz, M.A. Morse, et al., Nivolumab in patients with metastatic DNA mismatch repair-deficient or microsatellite instability-high colorectal cancer (CheckMate 142): an open-label, multicentre, phase 2 study, Lancet Oncol. 18 (9) (2017) 1182–1191.
[8] D.T. Le, J.N. Uram, H. Wang, B.R. Bartlett, H. Kemberling, A.D. Eyring, et al., PD-1 blockade in tumors with mismatch-repair deficiency, N. Engl. J. Med. 372 (26) (2015) 2509–2520.

[9] R.C. Wadlow, A.F. Hezel, T.A. Abrams, L.S. Blaszkowsky, C.S. Fuchs, M.H. Kulke, et al., Panitumumab in patients with KRAS wild-type colorectal cancer after progression on cetuximab, Oncol. 17 (1) (2012) 14.

[10] C. Eccleston, T.E. Cooper, E. Fisher, B. Anderson, N.M. Wilkinson, Non-steroidal anti-inflammatory drugs (NSAIDs) for chronic non-cancer pain in children and adolescents, Cochrane Database Syst. Rev. 8 (2017), CD012537.

[11] A. Ornelas, N. Zacharias-Millward, D.G. Menter, J.S. Davis, L. Lichtenberger, D. Hawke, et al., Beyond COX-1: the effects of aspirin on platelet biology and potential mechanisms of chemoprevention, Cancer Metastasis Rev. 36 (2) (2017) 289–303.

[12] E. Flossmann, P.M. Rothwell, British Doctors Aspirin T, the UKTIAAT. **Effect of aspirin on long-term risk of colorectal cancer: consistent evidence from randomised and observational studies,** Lancet 369 (9573) (2007) 1603–1613.

[13] P.M. Rothwell, M. Wilson, C.E. Elwin, B. Norrving, A. Algra, C.P. Warlow, et al., Long-term effect of aspirin on colorectal cancer incidence and mortality: 20-year follow-up of five randomised trials, Lancet 376 (9754) (2010) 1741–1750.

[14] X. Shen, X. Shen, A potential role for aspirin in the prevention and treatment of cholangiocarcinoma, Int. J. Cancer 148 (6) (2021) 1323–1330.

[15] W. Jiang, Y. Yan, M. Chen, G. Luo, J. Hao, J. Pan, et al., Aspirin enhances the sensitivity of colon cancer cells to cisplatin by abrogating the binding of NF-kappaB to the COX-2 promoter, Aging (Albany NY) 12 (1) (2020) 611–627.

[16] N. Huang, D. Chen, X. Wu, X. Chen, X. Zhang, J. Niu, et al., Aspirin promotes oligodendroglial differentiation through inhibition of Wnt signaling pathway, Mol. Neurobiol. 53 (5) (2016) 3258–3266.

[17] M.K. Gala, A.T. Chan, Molecular pathways: aspirin and Wnt signaling-a molecularly targeted approach to cancer prevention and treatment, Clin. Cancer Res. 21 (7) (2015) 1543–1548.

[18] H. Li, L. Li, B. Song, Q. Lin, X. Zhang, X. Lin, Aspirin inhabits proliferation and promotes apoptosis of pancreatic cancer cells via PI3K/Akt/mTOR signaling pathway, Panminerva Med. (2019), https://doi.org/10.23736/S0031-0808.19.03752-2.

[19] F. Lin, P. Zhang, Z. Zuo, F. Wang, R. Bi, W. Shang, et al., Thioredoxin-1 promotes colorectal cancer invasion and metastasis through crosstalk with S100P, Cancer Lett. 401 (2017) 1–10.

[20] X. Liao, P. Lochhead, R. Nishihara, T. Morikawa, A. Kuchiba, M. Yamauchi, et al., Aspirin use, tumor PIK3CA mutation, and colorectal-cancer survival, N. Engl. J. Med. 367 (17) (2012) 1596–1606.

[21] S.J. Dixon, K.M. Lemberg, M.R. Lamprecht, R. Skouta, E.M. Zaitsev, C.E. Gleason, et al., Ferroptosis: an iron-dependent form of nonapoptotic cell death, Cell 149 (5) (2012) 1060–1072.

[22] W.S. Yang, R. SriRamaratnam, M.E. Welsch, K. Shimada, R. Skouta, V. S. Viswanathan, et al., Regulation of ferroptotic cancer cell death by GPX4, Cell 156 (1–2) (2014) 317–331.

[23] Y. Li, X. Wang, Z. Huang, Y. Zhou, J. Xia, W. Hu, et al., CISD3 inhibition drives cystine-deprivation induced ferroptosis, Cell Death Dis. 12 (9) (2021) 839.

[24] F. Ursini, M. Maiorino, Lipid peroxidation and ferroptosis: the role of GSH and GPx4, Free Radic. Biol. Med. 152 (2020) 175–185.

[25] K. Bersuker, J.M. Hendricks, Z. Li, L. Magtanong, B. Ford, P.H. Tang, et al., The CoQ oxidoreductase FSP1 acts parallel to GPX4 to inhibit ferroptosis, Nature 575 (7784) (2019) 688–692.

[26] Z. Pei, Y. Liu, S. Liu, W. Jin, Y. Luo, M. Sun, et al., FUNDC1 insufficiency sensitizes high fat diet intake-induced cardiac remodeling and contractile anomaly through ACSL4-mediated ferroptosis, Metabolism 122 (2021), 154840.

[27] Y. Zou, H. Li, E.T. Graham, A.A. Deik, J.K. Eaton, W. Wang, et al., Cytochrome P450 oxidoreductase contributes to phospholipid peroxidation in ferroptosis, Nat. Chem. Biol. 16 (3) (2020) 302–309.

[28] X. Jiang, B.R. Stockwell, M. Conrad, Ferroptosis: mechanisms, biology and role in disease, Nat. Rev. Mol. Cell Biol. 22 (4) (2021) 266–282.

[29] C. Liang, X. Zhang, M. Yang, X. Dong, Recent progress in ferroptosis inducers for cancer therapy, Adv. Mater. 31 (51) (2019), e1904197.

[30] L. Mahoney-Sanchez, H. Bouchaoui, S. Ayton, D. Devos, J.A. Duce, J.C. Devedjian, Ferroptosis and its potential role in the physiopathology of Parkinson's Disease, Prog. Neurobiol. 196 (2021), 101890.

[31] F. Deng, B.C. Zhao, X. Yang, Z.B. Lin, Q.S. Sun, Y.F. Wang, et al., The gut microbiota metabolite capsiate promotes Gpx4 expression by activating TRPV1 to inhibit intestinal ischemia reperfusion-induced ferroptosis, Gut Microb. 13 (1) (2021) 1–21.

[32] Y. Li, D. Feng, Z. Wang, Y. Zhao, R. Sun, D. Tian, et al., Ischemia-induced ACSL4 activation contributes to ferroptosis-mediated tissue injury in intestinal ischemia/reperfusion, Cell Death Differ. 26 (11) (2019) 2284–2299.

[33] J. Lee, J.H. You, M.S. Kim, J.L. Roh, Epigenetic reprogramming of epithelial-mesenchymal transition promotes ferroptosis of head and neck cancer, Redox Biol. 37 (2020), 101697.

[34] J. Wu, A.M. Minikes, M. Gao, H. Bian, Y. Li, B.R. Stockwell, et al., Intercellular interaction dictates cancer cell ferroptosis via NF2-YAP signalling, Nature 572 (7769) (2019) 402–406.

[35] J.P. Thiery, Epithelial-mesenchymal transitions in tumour progression, Nat. Rev. Cancer 2 (6) (2002) 442–454.

[36] R. Gao, R.K.R. Kalathur, M. Coto-Llerena, D. Ercan, D. Buechel, S. Shuang, et al., YAP/TAZ and ATF4 drive resistance to Sorafenib in hepatocellular carcinoma by preventing ferroptosis, EMBO Mol. Med. 13 (12) (2021), e14351.

[37] J. Yang, J. Mo, J. Dai, C. Ye, W. Cen, X. Zheng, et al., Cetuximab promotes RSL3-induced ferroptosis by suppressing the Nrf2/HO-1 signalling pathway in KRAS mutant colorectal cancer, Cell Death Dis. 12 (11) (2021) 1079.

[38] P. Chen, X. Li, R. Zhang, S. Liu, Y. Xiang, M. Zhang, et al., Combinative treatment of beta-elemene and cetuximab is sensitive to KRAS mutant colorectal cancer cells by inducing ferroptosis and inhibiting epithelial-mesenchymal transformation, Theranostics 10 (11) (2020) 5107–5119.

[39] Y. Xia, S. Liu, C. Li, Z. Ai, W. Shen, W. Ren, et al., Discovery of a novel ferroptosis inducer-talaroconvolutin A-killing colorectal cancer cells in vitro and in vivo, Cell Death Dis. 11 (11) (2020) 988.

[40] J. Yi, J. Zhu, J. Wu, C.B. Thompson, X. Jiang, Oncogenic activation of PI3K-AKT-mTOR signaling suppresses ferroptosis via SREBP-mediated lipogenesis, Proc. Natl. Acad. Sci. U. S. A. 117 (49) (2020) 31189–31197.

[41] K. Duvel, J.L. Yecies, S. Menon, P. Raman, A.I. Lipovsky, A.L. Souza, et al., Activation of a metabolic gene regulatory network downstream of mTOR complex 1, Mol. Cell 39 (2) (2010) 171–183.

[42] R. Mancini, A. Noto, M.E. Pisanu, C. De Vitis, M. Maugeri-Sacca, G. Ciliberto, Metabolic features of cancer stem cells: the emerging role of lipid metabolism, Oncogene 37 (18) (2018) 2367–2378.

[43] H. Hua, H. Zhang, Q. Kong, J. Wang, Y. Jiang, Complex roles of the old drug aspirin in cancer chemoprevention and therapy, Med. Res. Rev. 39 (1) (2019) 114–145.

[44] X.R. Xu, G.M. Yousef, H. Ni, Cancer and platelet crosstalk: opportunities and challenges for aspirin and other antiplatelet agents, Blood 131 (16) (2018) 1777–1789.

[45] W.S. Henry, T. Laszewski, T. Tsang, F. Beca, A.H. Beck, S.S. McAllister, et al., Aspirin suppresses growth in PI3K-mutant breast cancer by activating AMPK and inhibiting mTORC1 signaling, Cancer Res. 77 (3) (2017) 790–801.

[46] M.J. Sanaei, A. Baghery Saghchy Khorasani, A. Pourbagheri-Sigaroodi, S. Shahrokh, M.R. Zali, D. Bashash, The PI3K/Akt/mTOR axis in colorectal cancer: oncogenic alterations, non-coding RNAs, therapeutic opportunities, and the emerging role of nanoparticles, J. Cell. Physiol. (2021) 1720–1752.

[47] G. Lech, R. Slotwinski, M. Slodkowski, I.W. Krasnodebski, Colorectal cancer tumour markers and biomarkers: recent therapeutic advances, World J. Gastroenterol. 22 (5) (2016) 1745–1755.

[48] J. Yang, J. Nie, X. Ma, Y. Wei, Y. Peng, X. Wei, Targeting PI3K in cancer: mechanisms and advances in clinical trials, Mol. Cancer 18 (1) (2019) 26.

[49] S. Uddin, M. Ahmed, A. Hussain, L. Assad, F. Al-Dayel, P. Bavi, et al., Cyclooxygenase-2 inhibition inhibits PI3K/AKT kinase activity in epithelial ovarian cancer, Int. J. Cancer 126 (2) (2010) 382–394.

[50] S.A. Glynn, R.L. Prueitt, L.A. Ridnour, B.J. Boersma, T.M. Dorsey, D.A. Wink, et al., COX-2 activation is associated with Akt phosphorylation and poor survival in ER-negative, HER2-positive breast cancer, BMC Cancer 10 (2010).

[51] J.M. Yi, J.J. Zhu, J. Wu, C.B. Thompson, X.J. Jiang, Oncogenic activation of PI3K-AKT-mTOR signaling suppresses ferroptosis via SREBP-mediated lipogenesis, P Natl. Acad. Sci. USA 117 (49) (2020) 31189–31197.

[52] G. Lei, L. Zhuang, B. Gan, mTORC1 and ferroptosis: regulatory mechanisms and therapeutic potential, Bioessays 43 (8) (2021), e2100093.

[53] Y. Baba, J.K. Higa, B.K. Shimada, K.M. Horiuchi, T. Suhara, M. Kobayashi, et al., Protective effects of the mechanistic target of rapamycin against excess iron and ferroptosis in cardiomyocytes, Am. J. Physiol. Heart Circ. Physiol. 314 (3) (2018) H659–H668.

[54] Y. Zhang, R.V. Swanda, L. Nie, X. Liu, C. Wang, H. Lee, et al., mTORC1 couples cyst (e)ine availability with GPX4 protein synthesis and ferroptosis regulation, Nat. Commun. 12 (1) (2021) 1589.

[55] A. Aljohani, M.I. Khan, D.N. Syed, B. Abram, S. Lewis, L.O. Neill, et al., Hepatic Stearoyl-CoA desaturase-1 deficiency-mediated activation of mTORC1- PGC-1alpha axis regulates ER stress during high-carbohydrate feeding, Sci. Rep. 9 (1) (2019), 15761.

[56] H. Shimano, R. Sato, SREBP-regulated lipid metabolism: convergent physiology - divergent pathophysiology, Nat. Rev. Endocrinol. 13 (12) (2017) 710–730.

[57] W. Eid, K. Dauner, K.C. Courtney, A. Gagnon, R.J. Parks, A. Sorisky, et al., mTORC1 activates SREBP-2 by suppressing cholesterol trafficking to lysosomes in mammalian cells, Proc. Natl. Acad. Sci. U. S. A. 114 (30) (2017) 7999–8004.

[58] F. Geng, X. Cheng, X. Wu, J.Y. Yoo, C. Cheng, J.Y. Guo, et al., Inhibition of SOAT1 suppresses glioblastoma growth via blocking SREBP-1-mediated lipogenesis, Clin. Cancer Res. 22 (21) (2016) 5337–5348.

[59] A. Talebi, J. Dehairs, F. Rambow, A. Rogiers, D. Nittner, R. Derua, et al., Sustained SREBP-1-dependent lipogenesis as a key mediator of resistance to BRAF-targeted therapy, Nat. Commun. 9 (1) (2018) 2500.

[60] C. Xu, L. Zhang, D. Wang, S. Jiang, D. Cao, Z. Zhao, et al., Lipidomics reveals that sustained SREBP-1-dependent lipogenesis is a key mediator of gefitinib-acquired resistance in EGFR-mutant lung cancer, Cell Death Dis. 7 (1) (2021) 353.

[61] M.T. Nakamura, T.Y. Nara, Gene regulation of mammalian desaturases, Biochem. Soc. Trans. 30 (Pt 6) (2002) 1076–1079.

[62] J. Liu, F. Kuang, G. Kroemer, D.J. Klionsky, R. Kang, D. Tang, Autophagy-dependent ferroptosis: machinery and regulation, Cell Chem. Biol. 27 (4) (2020) 420–435.

[63] C. Wang, M. Shi, J. Ji, Q. Cai, Q. Zhao, J. Jiang, et al., Stearoyl-CoA desaturase 1 (SCD1) facilitates the growth and anti-ferroptosis of gastric cancer cells and predicts poor prognosis of gastric cancer, Aging (Albany NY) 12 (15) (2020) 15374–15391.

[64] C.A. Wohlhieter, A.L. Richards, F. Uddin, C.H. Hulton, A. Quintanal-Villalonga, A. Martin, et al., Concurrent mutations in STK11 and KEAP1 promote ferroptosis protection and SCD1 dependence in lung cancer, Cell Rep. 33 (9) (2020), 108444.

[65] L. Magtanong, P.J. Ko, M. To, J.Y. Cao, G.C. Forcina, A. Tarangelo, et al., Exogenous monounsaturated fatty acids promote a ferroptosis-resistant cell state, Cell Chem. Biol. 26 (3) (2019) 420–432.